

the predicted lifetimes serves to validate this treatment and points to the presence of competing nonradiative channels in the few compounds that exhibit anomalously short lifetimes.

**Acknowledgment.** We thank 3M Co. and Merck & Co. for financial support of this work and the M. H. Wrubel Computer Center (Indiana University) for computational time.

**Registry No.** 1, 113132-50-6; 2, 113159-94-7; 3, 113132-52-8; Cp\*<sub>2</sub>CeI(THF), 113132-51-7; {Li(OEt)<sub>2</sub>}[C<sub>5</sub>H<sub>5</sub>(SiMe<sub>3</sub>)<sub>2</sub>CeCl<sub>2</sub>],

113132-53-9; Cp\*<sub>2</sub>CeI, 106333-17-9; Cp\*<sub>2</sub>CeCl(THF), 111559-69-4; [Li(OEt)<sub>2</sub>][Cp\*<sub>2</sub>CeCl<sub>2</sub>], 102307-94-8; K[(COT)<sub>2</sub>Ce], 51187-43-0; Cp\*<sub>2</sub>CeI<sub>2</sub>(THF)<sub>3</sub>, 105472-89-7; Ce(OSO<sub>2</sub>CF<sub>3</sub>)<sub>3</sub>, 76089-77-5.

**Supplementary Material Available:** Tables of crystal and diffractometer data, positional and thermal parameters, and bond distances and angles, a listing of the standard data tape, and various diagrams detailing the structure of **3** (12 pages); a listing of observed and calculated structure factors (3 pages). Ordering information is given on any current masthead page.

Contribution from the Departments of Chemistry, Principia College, Elmhurst, Illinois 62028, and Franklin and Marshall College, Lancaster, Pennsylvania 17604

## Specular Reflectance Spectra of Mixed-Metal Tetracyanide Salts: Nature of In-Plane Transitions in Ni(CN)<sub>4</sub><sup>2-</sup>

Gisela A. Arndt,<sup>1a</sup> Eric D. Danielson,<sup>1a</sup> Alan D. Fanta,<sup>1a</sup> and Ronald L. Musselman\*<sup>1</sup>

Received September 23, 1987

The polarized single-crystal specular reflectance spectra of a series of barium salts of Ni(CN)<sub>4</sub><sup>2-</sup>, Pt(CN)<sub>4</sub><sup>2-</sup>, and mixtures of the two complex anions show that the in-plane spectra behave differently for transitions originating on the two complexes. The interpretation is that the lowest energy Ni and Pt complex transitions polarized in-plane are not orbitally identical and that a new assignment of b<sub>2g</sub>(xy) → e<sub>u</sub>(π\*) for the low-energy <sup>1</sup>E<sub>u</sub> ← <sup>1</sup>A<sub>1g</sub> transition in Ni(CN)<sub>4</sub><sup>2-</sup> is required.

### Introduction

Solid-state tetracyano complexes of nickel(II), palladium(II), and platinum(II) have been of considerable interest because of the one-dimensional nature of the major electronic effects,<sup>2</sup> the potential superconductivity among one-dimensional conductors,<sup>3</sup> and the inherent interest due to the dramatic spectral changes upon crystallization from solution (the "solid-state effect").<sup>4-8</sup> Numerous electronic spectral studies have assigned observed absorptions to a variety of transitions with some general agreement in the Ni(CN)<sub>4</sub><sup>2-</sup> system<sup>9-12</sup> and less in the Pd(CN)<sub>4</sub><sup>2-</sup><sup>11,13,14</sup> and Pt(CN)<sub>4</sub><sup>2-</sup><sup>9,11-19</sup> systems. Both linear and circular polarization studies have determined the excited-state symmetries in many cases, but there is still ambiguity regarding actual orbital transitions. Our approach has been to add new dimensions to the available evidence by comparing single effects across several salts of a single metal complex as in (1) a series of Pd(CN)<sub>4</sub><sup>2-</sup> compounds in which a single-molecule origin of the prominent out-of-plane solid-state peak is identified,<sup>14</sup> (2) a single salt of three metalocyanides as with BaNi(CN)<sub>4</sub>, BaPd(CN)<sub>4</sub>, and BaPt(CN)<sub>4</sub>, in which the similarity of the out of plane solid-state peak is demonstrated across the series,<sup>20</sup> and (3) mixed-metal complexes as with [BaNi<sub>x</sub>Pt<sub>1-x</sub>(CN)<sub>4</sub>]<sub>4</sub>·4H<sub>2</sub>O, in which a delocalization over at least 20 centers was demonstrated for the prominent out-of-plane solid-state band.<sup>7</sup> In this work, we examine a more subtle aspect of these complexes, the lowest-energy in-plane bands in the barium salts of mixed Ni(CN)<sub>4</sub><sup>2-</sup> and Pt(CN)<sub>4</sub><sup>2-</sup>, which possess a significant amount of solid-state perturbation but do not lead to changes in color nor to one-dimensional conductivity. This has led to the need for a reevaluation of assignments for the lowest energy E<sub>u</sub> transition in Ni(CN)<sub>4</sub><sup>2-</sup>.

### Experimental Section

We have studied the in-plane polarized visible and ultraviolet reflection spectra of crystals prepared from a range of mixed aqueous solutions of barium tetracyanonickelate(II) and barium tetracyanoplatinate(II). The parent crystals are isomorphous, with space group C2/c, stacking perpendicular to the square planes and a M-M distance in the range of 3.32-3.36 Å.<sup>21,22</sup> We have assumed that the mixed crystals have similar structures; our polarized spectra have confirmed that the planar orientations are the same for both pure and mixed-metal crystals.

Single crystals of Ba[Ni<sub>x</sub>Pt<sub>1-x</sub>(CN)<sub>4</sub>]<sub>4</sub>·4H<sub>2</sub>O were grown from aqueous solutions ranging from 1:4 to 4:1 molar concentration of the pure Ba[M-

(CN)<sub>4</sub>]<sub>4</sub>·4H<sub>2</sub>O salts. BaPt(CN)<sub>4</sub>·4H<sub>2</sub>O was obtained by recrystallization from aqueous solution of the material from Ventron Chemicals. Ba[Ni(CN)<sub>4</sub>]<sub>4</sub>·4H<sub>2</sub>O was obtained by the combination of an excess of barium acetate with K<sub>2</sub>Ni(CN)<sub>4</sub>. The latter had been obtained by recrystallization from material from Research Inorganic/Organic Chemical Corp. Depending upon the concentration, the long well-formed needles resembled the green body color with blue-white reflectivity of Ba[Pt(CN)<sub>4</sub>]<sub>4</sub>·4H<sub>2</sub>O, the orange body with white reflectivity of Ba[Ni(CN)<sub>4</sub>]<sub>4</sub>·4H<sub>2</sub>O, or an intermediate appearance. The surface quality was preserved

- (1) (a) Principia College. (b) Franklin and Marshall College.
- (2) For reviews see: (a) Interrante, L. V., Ed. *Extended Interactions Between Metal Ions in Transition Metal Complexes*; ACS Symposium Series 5; American Chemical Society: Washington, DC, 1974. (b) Keller, H. J., Ed. *Low-Dimensional Cooperative Phenomena. The Possibility of High-Temperature Superconductivity*; Plenum: New York, 1975. (c) Keller, H. J., Ed. *Chemistry and Physics of One-Dimensional Metals*; Plenum: New York, 1977. (d) Miller, J. S., Epstein, A. J., Eds. *Syntheses and Properties of Low-Dimensional Materials*; Annals of the New York Academy of Sciences 313; New York Academy of Sciences: New York, 1978. (e) Devresse, J. T., Evrard, R., van Doren, V. E., Eds. *Highly Conducting One-Dimensional Solids*; Plenum: New York, 1979. (f) Miller, J. S., Ed. *Extended Linear Chain Compounds*; Plenum: New York, 1981; Vols. I and II. 1983; Vol. III. (g) King, R. B., Ed. *Inorganic Compounds with Unusual Properties*, Advances in Chemistry 150; American Chemical Society: Washington, DC, 1976. (h) King, R. B., Ed. *Inorganic Compounds with Unusual Properties—II*; Advances in Chemistry 173; American Chemical Society: Washington, DC, 1979.
- (3) (a) Little, W. A. *Phys. Rev. A* **1964**, *134*, 1416. (b) Gutfreund, H.; Little, W. A. In ref 2e, p 305.
- (4) Gmelin, L. *Jahrb. Chem. Phys.* **1822**, *36*, 230.
- (5) Day, P. J. *Am. Chem. Soc.* **1975**, *97*, 1588.
- (6) Moreau-Colin, M. L. *Struct. Bonding (Berlin)* **1972**, *10*, 167.
- (7) Anex, B. G.; Musselman, R. L. *J. Phys. Chem.* **1980**, *84*, 883.
- (8) Gliemann, G.; Yersin, H. *Struct. Bonding (Berlin)* **1985**, *62*, 87.
- (9) Piepho, S. B.; Schatz, P. N.; McCaffery, A. J. *J. Am. Chem. Soc.* **1969**, *91*, 5994.
- (10) Cowman, C. D.; Ballhausen, C. J.; Gray, H. B. *J. Am. Chem. Soc.* **1973**, *95*, 7873.
- (11) Mason, W. R.; Gray, H. B. *J. Am. Chem. Soc.* **1968**, *90*, 5721.
- (12) Gray, H. B.; Ballhausen, C. J. *J. Am. Chem. Soc.* **1963**, *85*, 260.
- (13) Moncuit, C. *J. Chim. Phys. Phys.-Chim. Biol.* **1967**, *64*, 494.
- (14) Musselman, R. L.; Anex, B. G. *J. Phys. Chem.* **1987**, *91*, 4460.
- (15) Moncuit, C.; Poulet, H. *J. Phys. Radium* **1962**, *23*, 353.
- (16) (a) Interrante, L. V.; Messmer, R. P. *Chem. Phys. Lett.* **1974**, *26*, 225. (b) Interrante, L. V.; Messmer, R. P. In ref 2a, p 382.
- (17) Marsh, D. G.; Miller, J. S. *Inorg. Chem.* **1976**, *15*, 720.
- (18) Isci, H.; Mason, W. R. *Inorg. Chem.* **1975**, *14*, 905.
- (19) Cowman, C. D.; Gray, H. B. *Inorg. Chem.* **1976**, *15*, 2823.
- (20) Musselman, R. L.; Cornelius, J. B.; Trapp, R. M. *Inorg. Chem.* **1981**, *20*, 1931.
- (21) Larsen, F. K.; Hazell, R. G.; Rasmussen, S. E. *Acta Chem. Scand.* **1969**, *23*, 61.
- (22) Maffly, R. L.; Johnson, P. L.; Williams, J. M. *Acta Crystallogr., Sect. B: Struct. Crystallogr. Cryst. Chem.* **1977**, *B33*, 884.

\* To whom correspondence should be addressed at Franklin and Marshall College.

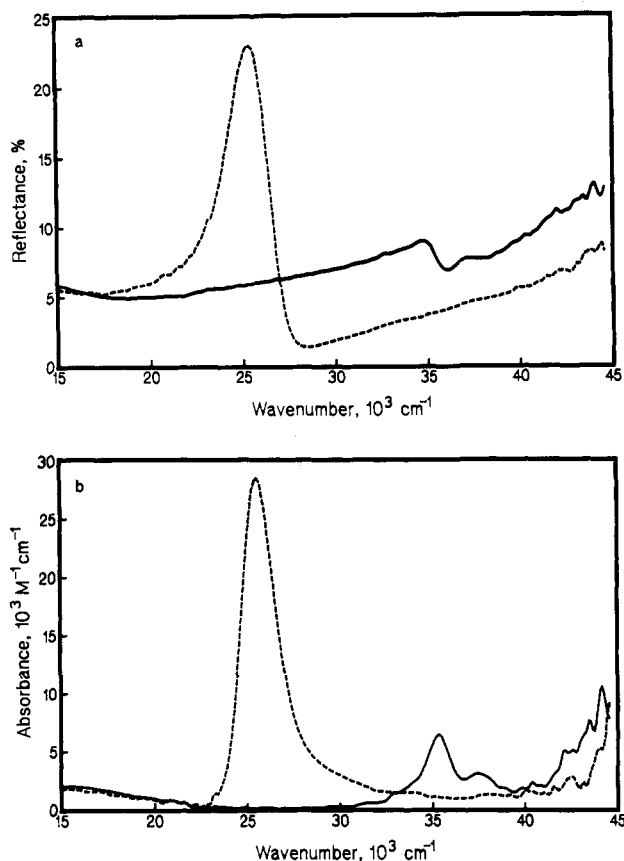


**Figure 1.** Polarized single-crystal spectra of  $\text{Ba}[\text{Ni}_{0.76}\text{Pt}_{0.24}(\text{CN})_4]\cdot 4\text{H}_2\text{O}$ . With the electric vector aligned parallel with the complex plane (in plane) (—) or perpendicular to the plane (out of plane) (---): (a) specular reflectance; (b) absorbance from Kramers–Kronig transformation of reflectance data.

by maintaining the atmosphere at 58% humidity in a NaBr hygrosat or by approximating that atmosphere with damp wicks near the crystals during reflection spectroscopy.

The reflection spectra were obtained on a double-beam specular reflectance instrument described in detail elsewhere<sup>23</sup> and based upon an earlier single-beam design.<sup>24</sup> The instrument was centered around a reflecting microscope and was controlled by an Apple IIe computer. Crystal surface regions with diameters as small as 30  $\mu\text{m}$  could be chosen for reflectance to ensure the best possible surface for measurement. The signal was evaluated statistically and collection continued until a 99% probability of a 1% agreement between the sample average and population average had been achieved. Spectra were obtained with the electric vector of the incident light aligned out-of-plane (parallel with the needle, or *c* crystallographic, axis) and in-plane (perpendicular to the needle axis). An internal reference beam mirror was calibrated to an NBS reflectance standard, yielding absolute reflectivities, which were transformed through a Kramers–Kronig analysis into absorptivities.<sup>24,25</sup> An effective transition was added in the vacuum UV to provide the reflectivity necessary for proper base-line behavior throughout the experimental region. The intensity of the high-energy tail of this effective band was adjusted to give as low an absorption as possible in the regions where the solution spectra show no intensity. This adjustment did not affect the energies of transformed absorption bands and had only minimal effect upon integrated intensities. The same effective transitions ( $\bar{\nu}_{R_{\text{max}}} = 53.9 \times 10^3 \text{ cm}^{-1}$ ,  $R_{\text{max}} = 33.4\%$ ) were used for all samples.

The composition of an individual crystal seldom equaled the composition of the solution from which it was crystallized due to the large difference in aqueous solubilities of  $\text{Ba}[\text{Ni}(\text{CN})_4]\cdot 4\text{H}_2\text{O}$  and  $\text{Ba}[\text{Pt}(\text{CN})_4]\cdot 4\text{H}_2\text{O}$ . Since during crystallization the composition of the solution changed, the composition of successive layers in a crystal also changed. As reflection spectroscopy is a near-surface process, the composition of the surface layers was of interest in our study and it was determined in this case by reference to a detailed study of the position of the low-energy

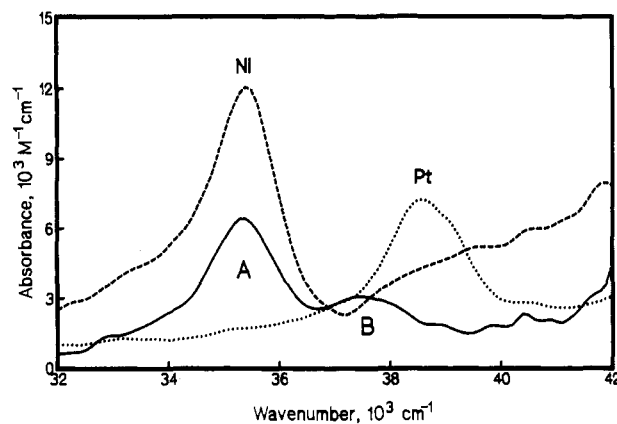


**Figure 2.** In-plane absorbance spectra from Kramers–Kronig transformation of  $\text{Ba}[\text{Ni}_{0.76}\text{Pt}_{0.24}(\text{CN})_4]\cdot 4\text{H}_2\text{O}$  (—),  $\text{Ba}[\text{Ni}(\text{CN})_4]\cdot 4\text{H}_2\text{O}$  (---), and  $\text{Ba}[\text{Pt}(\text{CN})_4]\cdot 4\text{H}_2\text{O}$  (···).

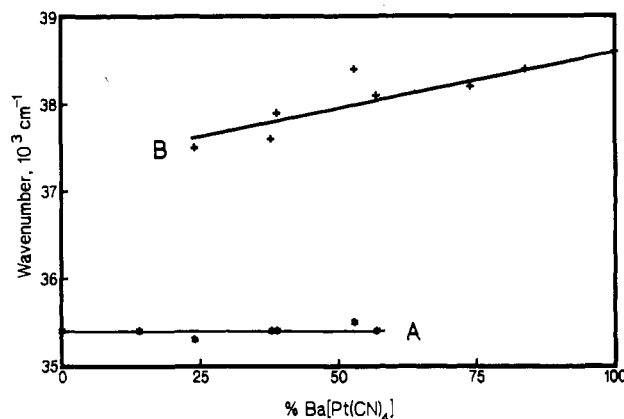


**Figure 3.** Relationships of positions of peaks A (\*) and B (+) with percent  $\text{Ba}[\text{Pt}(\text{CN})_4]\cdot 4\text{H}_2\text{O}$ .

out of plane peak vs  $\% \text{BaPt}(\text{CN})_4$ .<sup>7</sup>

### Results and Analysis

Single-crystal polarized specular reflectance spectra have been taken on 10 crystals ranging from  $\text{Ba}[\text{Ni}(\text{CN})_4]\cdot 4\text{H}_2\text{O}$  (0% Pt) to  $\text{Ba}[\text{Pt}(\text{CN})_4]\cdot 4\text{H}_2\text{O}$  (100% Pt) over the spectral range of 15 000 to 46 500  $\text{cm}^{-1}$ . The reflectance results for a typical crystal are shown in Figure 1a. Upon transformation via Kramers–Kronig analysis into absorption parameters, the spectra appear as in Figure 1b. The sharp peak at  $25.6 \times 10^3 \text{ cm}^{-1}$  was used in conjunction with Figure 3 of ref 7 to determine the surface composition to be  $24 \pm 3\% \text{ Ba}[\text{Pt}(\text{CN})_4]$ . A comparison of in-plane polarizations is given in Figure 2, which includes data for the 24% Pt crystal and pure  $\text{Ba}[\text{Ni}(\text{CN})_4]\cdot 4\text{H}_2\text{O}$  and  $\text{Ba}[\text{Pt}(\text{CN})_4]\cdot 4\text{H}_2\text{O}$  crystals. The mixed-metal crystal peak at  $35.3 \times 10^3 \text{ cm}^{-1}$  corresponds well with the pure  $\text{Ba}[\text{Ni}(\text{CN})_4]\cdot 4\text{H}_2\text{O}$  peak at  $35.4 \times 10^3 \text{ cm}^{-1}$  (peak A) and may thus be associated with it. The origin of the peak at  $37.5 \times 10^3 \text{ cm}^{-1}$ , however, is not as clear, although from the entire range of concentrations (vide infra), it may be seen to be associated with the  $\text{Ba}[\text{Pt}(\text{CN})_4]\cdot 4\text{H}_2\text{O}$  peak at  $38.6 \times 10^3 \text{ cm}^{-1}$  (peak B). It is also evident that the integrated intensities of peaks A and B have been reduced in the mixed crystal, from 0.196 and 0.076  $\text{\AA}^2$  to 0.075 and 0.0095  $\text{\AA}^2$ , respectively. Summaries of the data for the 10 crystals studied are presented as transition energies in Figure 3 and as integrated intensities in Figure 4.

The most immediate observation about the behavior of peaks A and B from the nickel and platinum salts is that they remain as two separate peaks upon mixing the complexes, in contrast to the prominent out-of-plane transitions.<sup>7</sup> In the latter, two distinct out-of-plane transitions for the tetracyanonickelate and tetracyanoplatinate salts at  $26.8 \times 10^3$  and  $23.3 \times 10^3 \text{ cm}^{-1}$ , respectively, became one peak of intermediate energy and intensity in mixed crystals. The origin of that peak appears to be the  ${}^1A_{2u} \leftarrow {}^1A_{1g} (a_{1g}(z^2) \rightarrow a_{2u}(\pi^*))$  transition in both the nickel and

(23) Desjardins, S. R.; Penfield, K. W.; Cohen, S. L.; Musselman, R. L.; Solomon, E. I. *J. Am. Chem. Soc.* **1983**, *105*, 4590.

(24) Anex, B. G. *Mol. Cryst.* **1966**, *1*, 1.

(25) Gottlieb, M. J. *Opt. Soc. Am.* **1960**, *50*, 343.

**Table I** Recent Assignments for Charge-Transfer Transitions in  $\text{Ni}(\text{CN})_4^{2-}$  and  $\text{Pt}(\text{CN})_4^{2-}$ 

$\text{Ni}(\text{CN})_4^{2-}$				
ref	method	a	A	C
this work	specular reflectance and soln abs	a 37 200 (13 040)		50 500
		b $^1E_u$		$^1E_u$
		c $e_g(xz,yz) \rightarrow e_u(\pi^*)$		$e_g(xz,yz) \rightarrow a_{2u}(\pi^*)$
Mason and Gray <sup>11</sup>	H <sub>2</sub> O CH <sub>3</sub> CN soln abs	a 37 300 (12 000)		50 000 (23 000)
		a' 36 230 (11 350)		
		b $^1E_u$		$^1E_{uII}$
		c $e_g(xz,yz) \rightarrow a_{2u}(\pi^*)$		$b_{2g}(xy) \rightarrow e_u(\pi^*)$
Peipho, Schatz, and McCaffery <sup>9</sup>	MCD	a 37 200 (11 400)		50 500
		b $A_{2u}1, E_u1$		$^1E_u$
Cowman, Ballhausen, and Gray <sup>10</sup>	5 K single-cryst abs [(n-C <sub>4</sub> H <sub>9</sub> ) <sub>4</sub> N] <sup>+</sup> salt	a 36 500 (VI); 36 700 (VII)		
		b $\left\{ \begin{array}{l} ^3E_u, ^3B_{1u} \text{ (VI); } ^1E_u \text{ (VII)} \\ ^3A_{2u}, ^1E_u \end{array} \right.$		
Demuyneck, Veillard, and Vinot <sup>27</sup>	LCAO-MO-SCF	a 37 900		46 900
		b $^1E_u$		$^1B_{1u}$
		c $e_g(xz,yz) \rightarrow a_{2u}(p_z, \pi^*)$		$b_{2g}(xy) \rightarrow a_{2u}(p_z, \pi^*)$
$\text{Pt}(\text{CN})_4^{2-}$				
ref	method	a	B	D
Gray and Ballhausen <sup>12</sup>	soln abs	a 39 180 (29 500)		
		b $^1E_u$		
		c $e_g(xz,yz) \rightarrow a_{2u}(\pi^*)$		
Moncuit <sup>13</sup>	soln abs	a 39 200 (10 600)		46 300 (22 600)
		b $^1E_u$		$^1E_u(\text{III}), ^1E_u(\text{IV})$
		c $e_g(xz,yz) \rightarrow a_{2u}(\pi^*)$		III: $b_{2g}(xy) \rightarrow e_u(\pi^*)$ IV: $e_g(xz,yz) \rightarrow b_{2u}(\pi^*)$
Mason and Gray <sup>11</sup>	soln abs	a 39 000 (9000)		46 190 (18 700)
		b $c^1E_u$		$d^1E_u$
		c $e_g(xz,yz) \rightarrow a_{2u}(\pi^*)$		$b_{2g}(xy) \rightarrow e_u(\pi^*)$
Peipho, Schatz, and McCaffery <sup>9</sup>	MCD	a 39 200 (10 700)		46 100 (22 100)
		b $E_u2, A_{2u}2$		$A_{2u}1, E_u1, B_{1u}1 (^3E_u)$
		c $e_g(xz,yz) \rightarrow a_{2u}(\pi^*)$		$b_{2g}(xy) \rightarrow e_u(\pi^*)$
Interrante and Messmer <sup>16</sup>	SCF-X $\alpha$ -SW	a 38 700		52 400
		b $E_u$		$E_u$
		c $e_g(xz,yz) \rightarrow a_{2u}(\pi^*)$		$e_u(\pi) \rightarrow a_{1g}(\sigma^*)$
Ischi and Mason <sup>18</sup>	MCD soln abs	a 38 450 (12 900)		45 500; 47 000
		b $A_{2u}1(^3Eu); Eu2(^3Eu)$		$A_{2u}2(^3Eu); E_u4(^3Eu) + \nu_{CN}$
Cowman and Gray <sup>19</sup>	polarized abs (n-Bu <sub>4</sub> N) <sub>2</sub> <sup>+</sup> salt	a 38 020; 38 880; 39 140		45 290; 45 700
		b $A_{2u}(^3E_u); E_u(^3E_u)$		$A_{2u}(^1A_{2u}); E_u(^1E_u)$

<sup>a</sup> Key: a, wavenumber in  $\text{cm}^{-1}$  (maximum absorbance in  $\text{M}^{-1} \text{cm}^{-1}$ ); b, state assignments,  $\leftarrow ^1A_{1g}$ ; c, orbital transitions corresponding to the  $E_u \leftarrow A_{1g}$  transitions listed in b, where available.

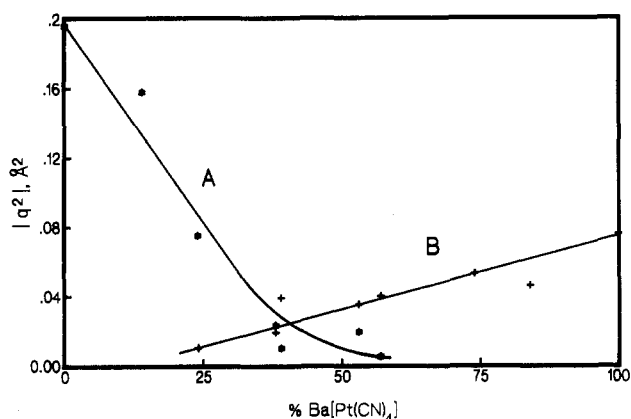


**Figure 4.** Integrated intensities of peaks A (\*) and B (+) as a function of percent  $\text{Ba}[\text{Pt}(\text{CN})_4] \cdot 4\text{H}_2\text{O}$ .

platinum complexes. That assignment seems reasonable in view of the demonstration of delocalization over at least 20 centers<sup>7</sup> and the proposals of band formation from the empty  $a_{2u}(\pi^*)$  orbitals, which has some  $p_z$  character, and from the filled  $a_{1g}$  orbitals of primarily  $d_{z^2}$  character.<sup>26</sup> Extended molecular orbitals or even bands would average the effective nuclear charge from each metal along a chain, thus giving a single intermediate value in the case of mixed-metal crystals. In the case at hand, however,

the two distinct peaks in the mixed-metal in-plane spectra indicate different behavior for the  $\text{Ni}(\text{CN})_4^{2-}$  and  $\text{Pt}(\text{CN})_4^{2-} \leftarrow ^1E_u \leftarrow ^1A_{1g}$  transitions.

It is important to next establish the origins of each of the transitions. Figure 4 illustrates that peak A increases in intensity with increasing  $\% \text{Ni}(\text{CN})_4^{2-}$  and that peak B increases in intensity with increasing  $\% \text{Pt}(\text{CN})_4^{2-}$ , thus indicating that peak A originates on  $\text{Ni}(\text{CN})_4^{2-}$  and peak B on  $\text{Pt}(\text{CN})_4^{2-}$ . This is, of course, confirmed in the pure materials. The significance in the mixed metals, however, is that the individual origins are retained throughout the range of concentrations.

The platinum-based peak B, which red-shifts over 1000  $\text{cm}^{-1}$  as the  $\% \text{Ni}$  content is increased, is reminiscent of the out-of-plane solid-state peak behavior. While the transition originates on Pt, the energy appears dependent upon the population of Ni centers surrounding the Pt. This behavior is consistent with the terminating orbital having a delocalized character. One such orbital, as noted in the review of out-of-plane spectra, is the  $a_{2u}(\pi^*, p_z)$  orbital. Table I illustrates that peak B has been widely assigned as the orbital transition,  $e_g(xz,yz) \rightarrow a_{2u}(\pi^*)$ . These assignments are consistent with our present observations.

Table I also shows that peak A, originating on  $\text{Ni}(\text{CN})_4^{2-}$ , has been assigned through experimental<sup>11</sup> and theoretical<sup>27</sup> bases as the same transition as the above peak in  $\text{Pt}(\text{CN})_4^{2-}$ . If this were the case, one would expect peaks A and B to both shift toward the other. The condition of a single peak would not necessarily

(26) Whangbo, M.-H.; Hoffmann, R. *J. Am. Chem. Soc.* **1978**, *100*, 6093.

(27) (a) Demuyneck, J.; Veillard, A.; Vinot, G. *Chem. Phys. Lett.* **1971**, *10*, 522. (b) Demuyneck, J.; Veillard, A. *Theoret. Chim. Acta* **1973**, *28*, 241.

be required since the overlap of the originating orbitals,  $d_{xz}$  and  $d_{yz}$ , is not as great as those for the solid-state  $A_{2u}$  transition,  $d_{z^2}$ , and limited overlap would not lead to identical ground state energies for the two complexes. Peak A, however, is notably energy stable throughout the range of concentrations for which it is observable, from 0 to 58% Pt. This energy stability demonstrates a clear independence from platinum, indicating that neither the originating nor terminal orbitals are participating in delocalization of any kind. This interpretation rules out the possibility of the  $e_g(xz,yz) \rightarrow a_{2u}(\pi^*)$  transition. A different assignment thus appears to be needed. The assignment should account for three factors: (1) no involvement with the delocalized orbital associated with the out-of-plane solid-state band, (2) solid-state red-shifting, since this band is of lower energy than its corresponding transition in solution, and (3) a reasonable alternate location for the  $e_g(xz,yz) \rightarrow a_{2u}(\pi^*)$  transition.

Possible candidates for peak A will be the several lowest energy  ${}^1E_u \leftarrow {}^1A_{1g}$  transitions in  $Ni(CN)_4^{2-}$ . Since spin-orbit coupling is not a major effect in  $Ni$ ,<sup>9</sup> only singlet-singlet transitions will be considered as bases for the state transitions. A widely accepted energy-level scheme is that of Gray and Ballhausen,<sup>12</sup> in which, for both  $Ni(CN)_4^{2-}$  and  $Pt(CN)_4^{2-}$ , the occupied metal d orbitals are distinct in energy from ligand orbitals. Although SCF-X $\alpha$ -SW calculations<sup>16</sup> on  $Pt(CN)_4^{2-}$  and  $[Pt(CN)_4^{2-}]_2$  show extensive mixing of both bonding and nonbonding ligand orbitals with metal d orbitals, which introduces many more choices for transitions, preliminary SCF-X $\alpha$ -SW calculations on  $Ni(CN)_4^{2-}$ <sup>28</sup> show a clear separation of metal d levels from bonding ligand orbitals. Thus, the most reasonable candidates for peak A will be the following transitions: (i)  $a_{1g}(z^2) \rightarrow e_u(\pi^*)$ ; (ii)  $b_{2g}(xy) \rightarrow e_u(\pi^*)$ ; (iii)  $e_g(xz,yz) \rightarrow b_{2u}(\pi^*)$ ; (iv)  $e_u(\pi^b) \rightarrow b_{1g}(x^2 - y^2)$ .

The third consideration noted earlier, an alternate location for the  $e_g(xz,yz) \rightarrow a_{2u}(\pi^*)$  transition, should now be discussed in preparation for considering the most likely assignment for peak A. Since we are ruling out this transition for peak A, it most likely will reside nearby in the low end of the remaining  $Ni(CN)_4^{2-}$  charge-transfer transitions. The second-lowest prominent  $E_u \leftarrow A_{1g}$  transition is at  $\sim 50\,500\text{ cm}^{-1}$  and appears to be the most likely location of  $e_g(xz,yz) \rightarrow a_{2u}(\pi^*)$ .

Peak A should thus be due to a transition of lower energy than  $e_g(xz,yz) \rightarrow a_{2u}(\pi^*)$ . This requirement eliminates transition iv since the  $b_{1g}(x^2 - y^2)$  orbital has been placed close to or above the  $a_{2u}(\pi^*)$  orbital<sup>12,16,26</sup> and  $e_u(\pi^b)$  is  $>1\text{ eV}$  below the occupied 3d levels.<sup>26</sup> Transition iii is also suspect since the  $b_{2u}(\pi^*)$  orbital

is nonbonding in the complex and most certainly is above the  $a_{2u}(\pi^*)$  orbital.

The remaining transitions, i and ii, are still plausible candidates on the basis of semiquantitative energy arguments. Transition i, however, is clearly associated with an orbital involved with the extensive out-of-plane delocalized transition,  $a_{1g}(z^2) \rightarrow a_{2u}(\pi^*)$ . Thus, the first consideration, noninvolvement with delocalized orbitals, rules out transition i. Transition ii thus passes the first and third considerations, and it also satisfies the second: a susceptibility to solid-state perturbation. While the mechanism of perturbations is not within the scope of this paper, it is reasonable to note that, though we have ruled out band formation for peak A in  $Ni(CN)_4^{2-}$ , both factor-group splitting<sup>29</sup> and crystal field interactions remain as other possible mechanisms. The latter could conceivably raise the energy levels of the  $3d_{xy}$  levels more than  $\pi_h^*$  levels due to the  $45^\circ$  staggering of adjacent planes<sup>21</sup> and the distance from Ni to the  $\pi_h^*$  orbitals, which would lead to red-shifting upon crystallization from solution. A solvent effect has been observed for this transition by Mason and Gray<sup>11</sup> in which they observed a  $1100\text{-cm}^{-1}$  red-shift upon changing the solvent from  $H_2O$  to  $CH_3CN$ .

The conclusions from our observations are that the in-plane  $35\,400\text{ cm}^{-1}$  transition in  $Ni(CN)_4^{2-}$  ( $37\,200\text{ cm}^{-1}$  in solution) is likely due to a  $b_{2g}(xy) \rightarrow e_u(\pi^*)$  orbital transition and the  $50\,500\text{ cm}^{-1}$  transition (C) is possibly the  $e_g(xz,yz) \rightarrow a_{2u}(\pi^*)$  transition. This essentially is a complete switch from two previous assignments<sup>11,13</sup> of the corresponding transitions in  $Pt(CN)_4^{2-}$ . Such a switch is not without some precedent: Peipho, Schatz, and McCaffery<sup>9</sup> have proposed that their assignment for the  $46\,100\text{-cm}^{-1}$   $Pt(CN)_4^{2-}$   $E_u$  transition (D) be applied to the  $37\,200\text{-cm}^{-1}$  transition in  $Ni(CN)_4^{2-}$  (A).

We are currently studying series of various salts of  $Ni(CN)_4^{2-}$  and  $Pt(CN)_4^{2-}$  and continuing SCF-X $\alpha$ -SW calculations on  $Ni(CN)_4^{2-}$  transitions to further elucidate the several effects apparently present in these compounds.

**Acknowledgment.** We are grateful for support of this work through grants from the Research Corp., The Camille and Henry Dreyfus Foundation, and the Illinois Philanthropic and Educational Foundation and for assistance in data collection from Annegret Schneider Zizza and Anne M. Barstow.

**Registry No.**  $Ba[Ni_{0.76}Pt_{0.24}(CN)_4] \cdot 4H_2O$ , 113273-47-5;  $Ba[Ni(CN)_4] \cdot 4H_2O$ , 17836-80-5;  $Ba[Pt(CN)_4] \cdot 4H_2O$ , 13755-32-3;  $[Ni(CN)_4]^{2-}$ , 48042-08-6;  $[Pt(CN)_4]^{2-}$ , 15004-88-3.

(28) Musselman, R. L.; Solomon, E. I., manuscript in preparation.

(29) Hochstrasser, R. M. *Molecular Aspects of Symmetry*; Benjamin: New York, 1966; Chapter 10.

Contribution from the Department of Chemistry, University of California, Los Angeles, California 90024-1569

## Excited-State Raman Spectroscopic Study of Bonding Changes in $K_3[Mn(CN)_5NO]$ Induced by Nitrosyl Bending

Jing-Huei Perng and Jeffrey I. Zink\*

Received July 30, 1987

The Raman spectrum of  $K_3[Mn(CN)_5NO]$  in the manganese to nitrosyl charge-transfer excited electronic state is reported. The CN stretching frequencies in the excited electronic state decrease by about  $100\text{ cm}^{-1}$  from those in the ground electronic state. The dependence of the Raman intensity on the laser pulse energy shows that the observed band arises from a two-photon process. Two excited-state Raman peaks are found in the metal-ligand region of the spectrum at  $533$  and  $565\text{ cm}^{-1}$  and are assigned to the excited-state MnCN bending mode and the Mn-N stretching mode, respectively. These peaks also exhibit a two-photon dependence on the laser pulse energy. The changes in the vibrational frequencies between the ground and excited electronic states are interpreted in terms of the loss of the highly covalent linear  $\{MNO\}^6$  unit caused by bending of the MNO bond in the excited electronic state.

Transition-metal nitrosyl complexes that contain a linear MNO unit can undergo a geometry change to a bent MNO unit in metal

to ligand charge-transfer excited states.<sup>1-3</sup> The photochemical consequences of this geometry change were first pointed out in